A High Performance Terahertz Waveguide Detector Based on a Low-Barrier Diode *

Tian-Hao Ren(任田昊)[1,2], Yong Zhang(张勇)[2**], Bo Yan(延波)[2], Rui-Min Xu(徐锐敏)[2], Cheng-Yue Yang(杨成樾)[1], Jing-Tao Zhou(周静涛)[1**], Zhi Jin(金智)[1**]

[1]*Department of Microwave IC, Institute of Microelectronics, Chinese Academy of Sciences, Beijing 100029*
[2]*School of Electronic Engineering, University of Electronic Science and Technology of China, Chengdu 611731*

(Received 7 March 2016)

A Schottky barrier diode with low-barrier is presented, based on which a terahertz waveguide detector working at 500–600 GHz is designed and fabricated. By using the InGaAs/InP material system, the feature of the low barrier is obtained which greatly improves the performance of the detector. The measured typical voltage responsivity is about 900 V/W at 500–560 GHz and is about 400 V/W at 560–600 GHz. The proposed broadband waveguide detector has the characteristics of simple structure, compact size, low cost and high performance, and can be used in a variety of applications such as imaging, molecular spectroscopy and atmospheric remote sensing.

PACS: 07.57.−c, 84.40.−x, 84.40.Az DOI: 10.1088/0256-307X/33/6/060701

Terahertz (THz) detection technology becomes more and more attractive for its applications in astronomy, imaging and bio-sensing.[1,2] Various kinds of detectors have been developed for different applications.[3] Schottky barrier diode (SBD) detectors have long been used in millimeter-wave (MMW) and THz regions due to their high sensitivity, ability to operate at an ambient or cryogenic temperature and fast response time. When the diodes are optimized to have a low forward turn-on voltage, the detectors can achieve excellent frequency response and bandwidth, even with zero bias. InGaAs/InP is verified to be a very promising material system for the detection at MMW and THz frequencies. Superior to the traditional material, such as GaAs, its lower Schottky barrier height provides zero-bias detection ability that not only eliminates shot noise and hence improves crucially signal-to-noise ratio but also simplifies the detection system.[4] In this work, an SBD with low-barrier is presented, based on which a terahertz waveguide detector working at 500–600 GHz is designed and fabricated.

A common structure of an SBD is depicted in Fig. 1. As mentioned above, detectors can achieve excellent frequency response and bandwidth based on SBDs with low forward turn-on voltage. Hence, the InGaAs/InP material system which has a low barrier height is selected. The doping levels and thicknesses of the epitaxial layer and buffer layer need to be carefully designed to meet the demand of the detector. To minimize the series parasitic resistance, the buffer doping concentration $N_{\rm buffer}$ is chosen to be as high as possible, such as $3\times10^{19}\,{\rm cm}^{-3}$. The thickness of the buffer layer, $t_{\rm buffer}$, should be larger than one skin depth at the working frequency, while larger thickness leads to larger cost. Thus $t_{\rm buffer}$ is chosen as 1.5 μm. The decisions of epitaxial doping concentration $N_{\rm epi}$ and epi-layer thickness $t_{\rm epi}$ are related to each other. Here $t_{\rm epi}$ should be slightly larger than the maximum depletion depth, which is related to $N_{\rm epi}$. The decision of $N_{\rm epi}$ is a compromise between series resistance and reverse breakdown voltage. Here $N_{\rm epi}$ and $t_{\rm epi}$ are chosen as $3\times10^{17}\,{\rm cm}^{-3}$ and 0.2 μm, respectively. The diameter of the Schottky contact is chosen as 1 μm to obtain a reasonable junction capacitance which satisfies the demand of the detector.

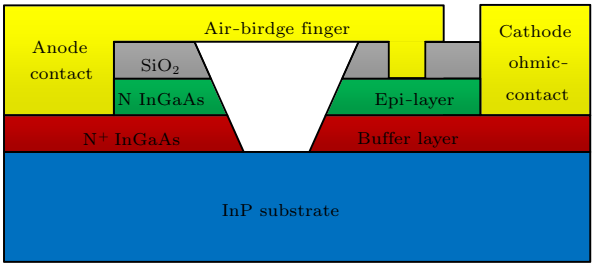

Fig. 1. Cross-sectional view of the SBD.

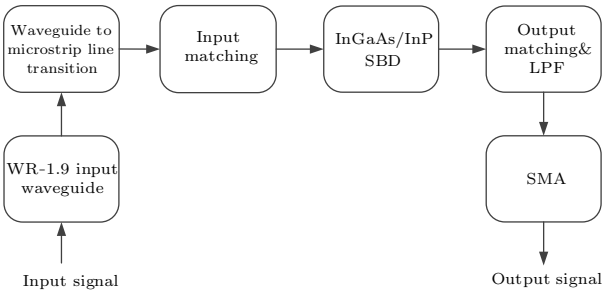

Fig. 2. The schematic diagram of the detector.

Generally, the detector can be divided into two parts, the linear part and the nonlinear part. The presented detector consists of six parts: input waveguide, waveguide to microstrip line transition, input matching, diode part, low pass filter (LPF) with output matching, and SMA, as shown in Fig. 2. Details about the design process are described in the follow-

*Supported by the National High-Technology Research and Development Program of China under Grant No 2011AA010203, the National Basic Research Program of China under Grant Nos 2011CB201704 and 2010CB327502, and the National Natural Science Foundation of China under Grant No 61434006.

**Corresponding author. Email: zhoujingtao@ime.ac.cn; jinzhi@ime.ac.cn; yongzhang@uestc.edu.cn

© 2016 Chinese Physical Society and IOP Publishing Ltd

ing.

The input waveguide is chosen as the WR-1.9 waveguide for the specific working frequencies. The waveguide to microstrip line transition is shown in Fig. 3(a). Note that a GND point is designed to provide a closed dc path where the detected dc signal could flow. The simulated reflection coefficient S_{11} is smaller than -19 dB and the transmission coefficient S_{21} is larger than -0.15 dB at 500–600 GHz, respectively, as shown in Fig. 3(b). The results indicate that the transition part could meet the requirement of the detector.

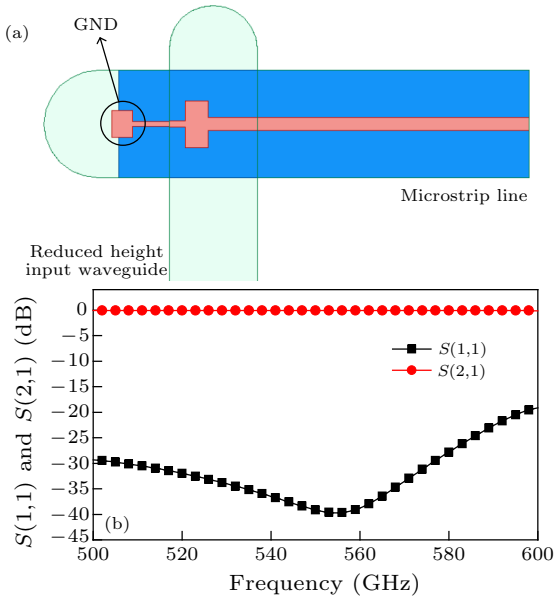

Fig. 3. Waveguide to microstrip line transition: (a) model and (b) simulated results.

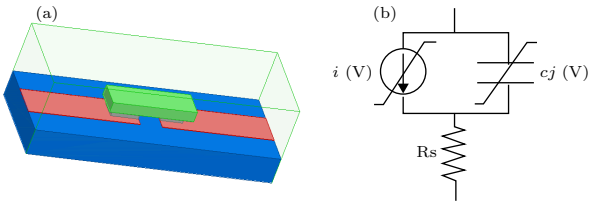

Fig. 4. (a) The 3D full wave simulation model of the diode parasitic part and (b) the nonlinear model of the Schottky junction.

Then we build the whole detector nonlinear model in Agilent's advanced design system (ADS) to find the optimized input matching, LPF and output matching. The goal is that the detector could achieve high voltage responsivity. To carry out this, we need to build the nonlinear model of the SBD first. Here we use a high-frequency structure simulator (HFSS) to build the 3D full wave simulation model of the linear parasitic part and the SPICE model in the ADS to build the intrinsic Schottky junction, respectively, as shown in Fig. 4.

The definition of wave port representing the entrance to the Schottky junction is very important to achieve a correct simulation, which is defined as a circular sheet between the epi-layer and the buffer layer with a perfect cylindrical conductor through the epi-layer, as shown in Fig. 5.

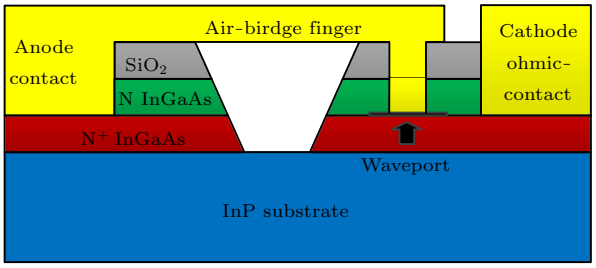

Fig. 5. Definition of the wave port.

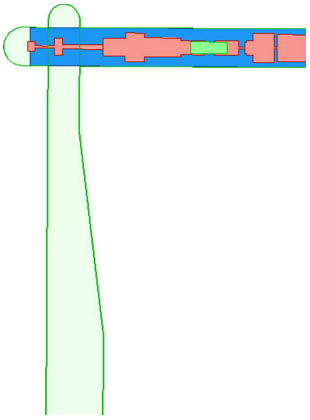

Fig. 6. The whole structure of the detector.

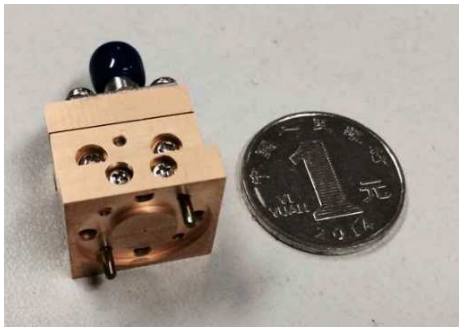

Fig. 7. Photograph of the detector.

After the optimization process, the initial structures of the input and output matching parts are obtained, which are then rebuilt in the HFSS to verify the simulated results for the operating frequency is very high (500–600 GHz). The models in the HFSS are modified to obtain the simulated results which are similar to those in the ADS. Finally, the whole detector is built in the HFSS, as shown in Fig. 6, and is simulated in the ADS. A photograph of the detector is shown in Fig. 7.

Voltage responsivity and noise equivalent power (NEP) are two important characteristics of detectors. Voltage responsivity can be described as

$$R_{\rm v} = \frac{V_{\rm out,dc}}{P_{\rm in,ac}}, \tag{1}$$

where $V_{\rm out,dc}$ is the magnitude voltage of the output dc signal, and $P_{\rm in,ac}$ is the power of the input ac signal. The terahertz source is obtained by frequency multiplier chain of VDI and its power is measured by a Golay cell detector. The terahertz signal is pumped into our broadband detector and then the dc signal is

measured by a phase-locked amplifier. The comparison between simulated and measured voltage responsivity of the detector is shown in Fig. 8. Except for the two resonance points around 500 and 555 GHz due to the cavities, the measured typical voltage responsivity is 900 V/W at 500–560 GHz and is about 400 V/W at 560–600 GHz, respectively. This difference is due to the larger loss at higher frequencies[5,6] (e.g., the series resistance of the diode becomes larger as the frequencies increase). There is also some deviation between the simulated and measured results, which may be due to the inaccurate simulation model, processing error and assembling error.

The NEP can be calculated by

$$\mathrm{NEP} = \frac{N_{\mathrm{v}}}{R_{\mathrm{v}}}, \tag{2}$$

where N_{v} is the noise voltage of the detector, which is measured by a noise analyzer. Commonly N_{v} is measured with zero rf power. Under this condition only thermal noise is generated, which is different from the actual condition. In fact, as the input power increases, excessive noise such as flicker noise is generated. Flicker noise becomes increasingly important as the input power is increased.[7] Here N_{v} is measured as 25×10^{-9} V/Hz$^{0.5}$. Then NEP is calculated, as shown in Fig. 9. Except for the two resonance points, the typical NEP is measured to be 27.78 pW/Hz$^{0.5}$ at 500–560 GHz and 62.5 pW/Hz$^{0.5}$ at 560–600 GHz.

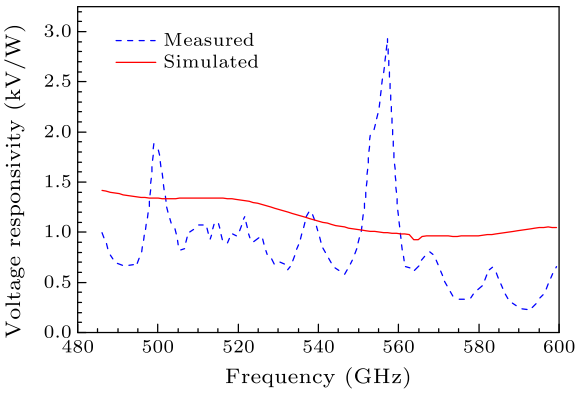

Fig. 8. Measured and simulated voltage responsivity of the detector.

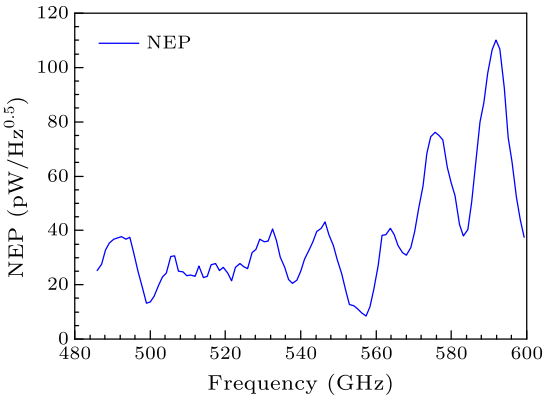

Fig. 9. The measured NEP of the detector.

Table 1. Comparison with other related works.

Reference	Working frequencies	Typical voltage responsivity	Remarks
Yao *et al.*[8]	110–170 GHz	600 V/W	GaAs
Zhang *et al.*[9]	260–280 GHz	1400 V/W	InP
Liu *et al.*[10]	150–400 GHz	300–1000 V/W	Quasi-optical
This work	500–600 GHz	400–900 V/W	InP

In Table 1, we list some related works about terahertz detectors based on SBDs. Compared with the related studies, the presented detector has the characteristics of high working frequencies, high performance and broad band.

In summary, the advantage of the InGaAs/InP material system is its low barrier height which leads to high responsivity and wide bandwidth of the detector. Utilizing the topology of zero bias, the proposed detector becomes simple, compact and low cost, while maintaining high performance. The measured typical voltage responsivity is about 900 V/W at 500–560 GHz and is about 400 V/W at 560–600 GHz. The typical NEP is measured to be 27.78 pW/Hz$^{0.5}$ at 500–560 GHz and 62.5 pW/Hz$^{0.5}$ at 560–600 GHz, respectively. Compared with other related works, our detector is the best SBD-based waveguide detector working at 500–600 GHz in China. The present detector has a variety of applications such as imaging, molecular spectroscopy and atmospheric remote sensing.

References

[1] Zmuidzinas J and Richards P L 2004 *Proc. IEEE* **92** 1597
[2] Woolard D L, Globus T R, Gelmont B L, Bykhovskaia M, Samuels A C, Cookmeyer D, Hesler J L, Crowe T W, Jensen J O, Jensen J L and Loerop W R 2002 *Phys. Rev.* E **65** 051903
[3] Tu X C, Kan L, Liu X H, Mao Q K, Wan C, Chen J, Jin B B, Ji Z M, Xu W W and Wu P H 2013 *Chin. Phys.* B **22** 040701
[4] Semenov A, Cojocari O, Hubers H W, Song F, Klushin A and Muller A S 2010 *IEEE Electron Device Lett.* **31** 674
[5] Maestrini A, Thomas B, Wang H, Jung C, Treuttel J, Jine Y, Chattopadhyay G, Mehdi I and Beaudin G 2010 *C. R. Phys.* **11** 480
[6] Chattopadhyay G 2011 *IEEE Trans. Terahertz Sci. Technol.* **1** 33
[7] Hesler J L and Crowe T W *2007 18th Intl. Symp. Space Terahertz Tech.* (Pasadena, CA) pp 89–92
[8] Yao C F, Zhou M, Luo Y S, Xu C H, Kou Y N and Chen Y G 2013 *Acta Electron. Sin.* **41** 438 (in Chinese)
[9] Zhang J J, Zhou J T, Yang C Y, Tian Z and Jin Z 2015 *J. Infrared Millimeter Waves* **34** 1
[10] Liu L, Hesler J L, Xu H Y, Lichtenberger A W and Weikle I R M 2010 *IEEE Microwave Wireless Compon. Lett.* **20** 504